

# Advanced Modelling Approach for ACT/FHS Controller Development

Mario Hamers  
Wolfgang von Grünhagen

Deutsches Zentrum für Luft- und Raumfahrt e.V. (DLR)  
Institute of Flight Research  
Braunschweig, Germany

## Abstract

The advanced airborne testbed FHS (Flying Helicopter Simulator), DLR's new in-flight simulator, will soon start into the flight testing phase for final certification issues. Basing on a Eurocopter EC135 helicopter the FHS is equipped by the manufacturer with a 4 times redundant fly-by-light control system as well as an experimental system developed by DLR which provides all necessary features required to operate the helicopter as an in-flight simulator.

DLR is preparing the first user applications to be conducted with FHS which not only will contribute to the certification flight tests but also allow to be used for first handling qualities investigations as soon as the FHS will be available to DLR and other users. A whole chain of tools and disciplines is involved in the development process of experimental control software. To give an overview of this process the present paper will especially highlight the efforts and progress in the helicopter modelling and system identification disciplines. Their application will be shown in the light of one of the first experimental applications i.e. bandwidth investigations by implementing a lead/lag filter in the pilot control feed forward.

## Notations

$a_{1,2}, b_{1,2}$	Wagner function coefficients, [-]
$a_s$	sound speed, [m/s]
$m, r, n, j$	harmonic and shape indices, [-]
$r$	non dimensional rotor radius, [-]
$s$	Laplace variable, [-]
$t$	time, [s]
$t^*$	reduced time, [-]
$w$	normal inflow velocity, [-]
$x, y$	input and output states, [-]
$D_{1,2}, W_{1,2}$	2 <sup>nd</sup> order system parameters, [-]
$F_{b,e}$	blade element lift force, [N]
$G$	controller gains, [-]

$H$	Legendre derivative function matrix, [-]
$L$	inflow gain matrices, [-]
$L_p, L_{\delta y}$	1 <sup>st</sup> order roll system coefficients, [1/s]
$M$	mass matrix, [-]
$M_{x,z,\infty}$	Mach numbers, [-]
$M_q, M_{\delta x}$	1 <sup>st</sup> order pitch system coefficients, [1/s]
$N_b$	number of blades, [-]
$N_e$	number of blade elements, [-]
$\bar{P}, \bar{Q}$	normalized associated Legendre functions of first and second kind, [-]
$R$	rotor radius, [m]
$T$	controller time constants, [s]
$U_\infty$	free stream velocity, [m/s]
$V$	flow matrix, [-]
$V_M$	non dimensional flow parameter, [-]
$V_T$	total flow parameter, [-]
$V_z$	normal inflow velocity, [m/s]
$\alpha, \beta$	induced inflow coefficients, [-]
$\alpha, \alpha_e$	angle of attack, [rad]
$\beta$	compressibility factor, [-]
$\delta$	switch function, [-]
$\delta_{ij}$	Kronecker symbol, [-]
$\phi_{step}$	Wagner function, [-]
$\lambda, \lambda_m$	inflow parameters, [-]
$\mu$	disk advance ratio, [-]
$\nu, \eta, \psi$	ellipsoidal coordinates, [-]
$\rho$	air density, [kg/m <sup>3</sup> ]
$\tau$	pressure coefficients, [-]
$\tau$	integration time parameter, [s]
$\tau_{p,d}$	time delays, [ms]
$\psi_b$	blade azimuth, [rad]
$\omega_{bw}$	bandwidth, [rad/s]
$\Phi$	non dimensional pressure potential, [-]
$\Omega$	rotor speed, [rad/s]
$\Psi$	radial shape function, [-]

## Introduction

In the whole development process of FHS in-flight simulation three research disciplines play a major role, i.e. non-linear modelling of the helicopter

dynamics, helicopter system identification and control system design. All three of them are tightly entwined with each other and base on a detailed system analysis. The results of one discipline are inputs for the others and vice versa. **Figure 1** shows the relations between modelling, system identification and the control system design in a condensed form.

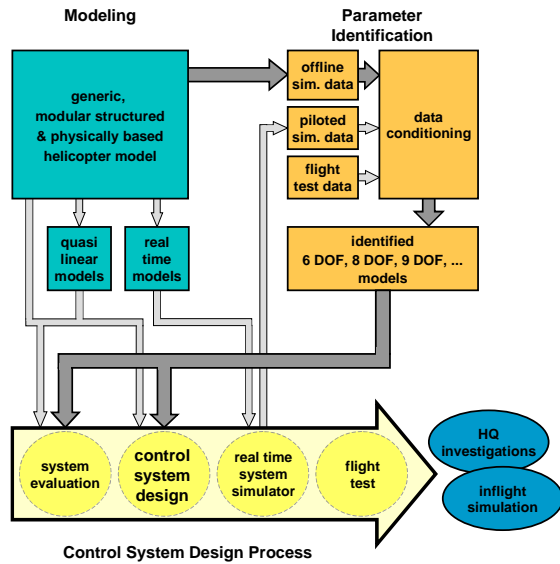


**Figure 1:** control system design process

As can be seen the outcome of the modelling activities find application in the control law design, the system identification as well as in the FHS system simulator under real time conditions. It is obvious that in order to reduce the costs arising from flight tests hours for adjusting and tuning parameters of the control system a highly accurate helicopter model suitable for pilot and hardware in-the-loop is indispensable. Especially, the simulation model bandwidth and coupling behaviour has to correspond with the controller bandwidth for a correct design of the latter. The paper will describe in detail model extensions to the dynamic inflow formulation taking into account unsteady aerodynamic effects in order to improve the helicopter cross-coupling prediction capability.

As can be seen from the identification block on the right hand side the origin of the data to be analysed is not of essential interest. Identification is done for flight test data, piloted simulation data as well as for off-line simulation data. Key issue for the identification performance is the quality and applicability of the data for its special purpose. Further, for the use in the helicopter control system design, with a special emphasis on the model following control (MFCS), the structure of the identified model is important. In this context typical

6 DOF rigid body models are extended with rotor degrees of freedom.

For the moment all three data input options as displayed in **figure 1** are applied, leading to a system of 6, 8 and 9 DOF identified models with different complexity, i.e. the number of states incorporated. The identified models from off-line simulated data find application especially in the beginning of the design process, since they relatively simple allow for parameter and configuration studies (e.g. stability margin estimation). However, when all necessary tools are made available and will be tested, in the final control system design for the flying system models identified from FHS flight test data will be used. In this paper the results of the system identification tool using off-line simulation data will be shown.

Industry partners will use the FHS mostly as a technology demonstrator, whereas for DLR the active control technology is the most interesting aspect. Here, the applications will vary from open loop techniques such as passive (e.g. gains) and active control (e.g. time dependant elements filters and delays) mixing of the pilot commands to the more demanding closed loop applications with in particular the model following control (MFCS) approach. The typical structure of the MFCS is shown in **figure 2**.

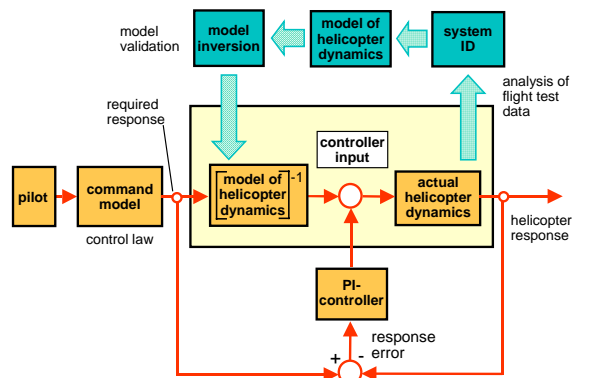


**Figure 2:** MFCS principal structure

The MFCS approach is used to investigate advanced controller systems, variations of basic handling qualities to finally simulate other helicopters in flight.

All active control applications make use of identified models (see e.g. **figure 2**). For the open loop applications 6 DOF models will normally be sufficient, whereas the MFCS application requires higher order 8 and 9 DOF models.

As an example of one of the first experimental open loop control applications a lead/lag filter as a pure

feed-forward on the pilot control inputs, equivalent to a bandwidth variation, in combination with cross feed gains, will be described in the present paper.

## FHS In-flight Simulator

To gain a better understanding of the FHS functionality, especially when used as an in-flight simulator a short overview of the system architecture is presented.

The FHS is designed to validate key technologies for future helicopters. For extending flight operations to a 24h all weather capability, new control technologies, cockpit design and man-machine interfaces will be investigated in-flight. In order to accomplish these tasks the FHS is equipped with a quadruplex fly-by-light control system. The on-board system consists of two associated units: the core system (COS) and the experimental system (ES).

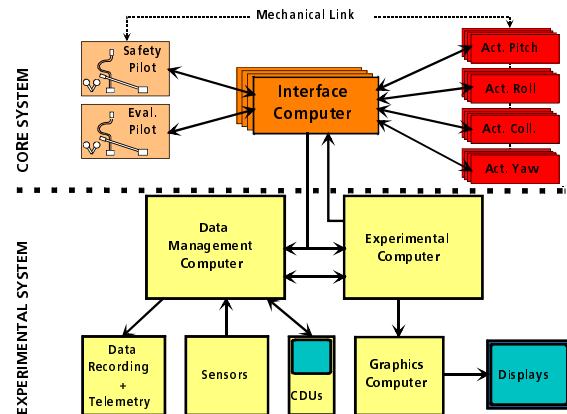


**Figure 3:** FHS system architecture

As depicted in **figure 3** the core system incorporates the 4 times redundant control system, whereas the experimental system is presently designed as a simplex system. The basic EC135 helicopter including the core system builds the basic FHS flying system, designed fail safe and meeting the high aviation safety standards. The experimental system is adaptable to the particular user program. A safe operation of the experimental system is guaranteed by the action of a safety pilot monitoring the overall system.

The COS (core system interface computer) unit is a quadruplex computer, which manages the fly-by-light data transfer from pilot controls to actuators and vice versa, as well as the transition between the different helicopter operating modes, for example: safety pilot in command, synchronisation of evaluation pilot controls, evaluation pilot in command, experimental mode, and finally switching back to the safety pilot command mode, either in

regular or in a safety critical case. A more extensive description of the FHS in-flight simulator is given in [1].

The particular user experiments (applications) run on the experimental computer. Data handling, recording and telemetry is managed by the DMC (data management computer).

## Modelling

Accurate dynamic helicopter models are needed at several levels of the control design process as shown in **figure 1**. In the FHS project the model development environment of the EC135 helicopter is SIMH, the real-time model development platform of DLR. In former presentations the performance of the flight dynamic behaviour prediction has been demonstrated, e.g. [2].

Due to the continual attempt to further improve the prediction capability of the models especially in identified problem areas three topics remain of interest:

1. improving the pitch-roll & roll-pitch cross-coupling response prediction capability by appropriate global dynamic inflow and local unsteady aerodynamics (using airfoil deficiency functions) formulations
2. accurate modelling of the highly complex aerodynamics and dynamics of the fenestron (fan-in-fin) in order to improve yaw response prediction
3. implementation of a dynamic model for the helicopter engines including the FADEC control system and drive train dynamics in order to improve the model accuracy in the prediction coupled heave / yaw / lead-lag behaviour.

With respect to the above topic 2, work at DLR is ongoing to extend the existing fenestron model to take account for the strongly non-linear local aerodynamics especially in forward flight. As shown in [3] the use of parameter optimisation tools in the above investigations produces promising results.

Since, for the moment very few data for the FADEC system and no dynamic data of the overall engine-FADEC system are available, investigations related to topic 3 will be postponed until the first FHS flight test campaign to generate validation data is completed.

In the following, the work related to topic 1 will be described. In order to improve the cross-coupling prediction in generic non-linear models in a co-operative DLR and ONERA work the finite state unsteady wake model was implemented in the simulation codes and validated [4], [5]. In addition,

several model extensions have been developed. From the experience gained with the application of this dynamic inflow formulation it was found a powerful and widely useable tool. As an example the upper two subplots in **figure 4** show the dynamic pressure and velocity distribution at the rotor disk for a EC135 helicopter in a 100 kts level flight as a snap shot. **Figure 4** also shows the contour plot (values evaluated during one rotor revolution at the blade stations only) of the induced velocity for the same case.

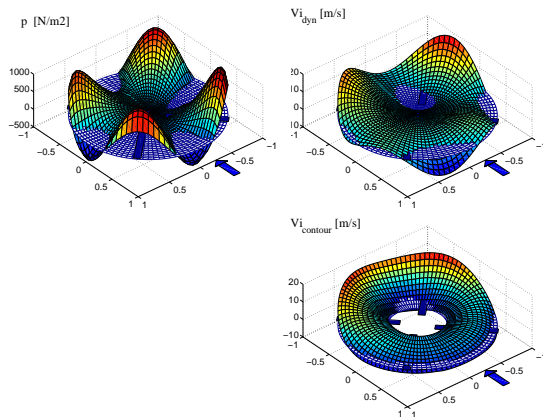


**Figure 4:** pressure and velocity distribution for EC135 in moderate forward level flight

The realistic representation of the induced up-wash velocity at the rotor front section can be clearly seen.

Since the finite state unsteady wake theory comprises the analytical solution of the Laplace equations, many aerodynamic effects are implicitly included in this formulation, especially unsteady aerodynamic wake effects. For example in [6] comparisons of the finite state unsteady wake model with other unsteady theories, as there are e.g. Theodorsen's theory, Loewy-Miller theory, show that the infinite unsteady wake formulation is able to recover these other theories. In the 2 D case it could be shown that it is even possible to improved the classical theories, as demonstrated by comparison with measured data.

The good agreement of the finite state unsteady wake theory with the classical unsteady theories is achieved especially for the axial flight case, i.e. hover or vertical climb or descent.

In DLR applications of the finite state unsteady wake theory, e.g. real-time realisation in the ground based system simulator for the FHS, only a limited number of states is used due to computation time constraints and also due to numerical stability of the integration scheme [4]. It was found that limiting the number of harmonics to 4 (resulting in a total

number of 15 states) represents a good compromise between above constraints and the achieved (and required) flight dynamic accuracy. Further, the balance between the complexity and thus the order of the blade dynamic description (rigid blades with second order flap and lead-lag) and the aerodynamic wake formulation should be guaranteed. Increasing only the order or number of states in either the dynamic or aerodynamic description does not improve the overall simulation fidelity as expected.

In the above described applications it is obvious that a steady hover or axial flight will only be the exception. Generally, more or less high dynamic manoeuvres in low speed as well as forward speed will be flown, thereby continuously exiting the dynamic inflow system. For these high dynamic helicopter and rotor motions the finite state unsteady wake approach is not able to catch all unsteady effects originating from shed vortex interaction especially when the formulation is used with a limited number of harmonics and states.

Unsteady local blade aerodynamic effects in terms of a time delay or lead-lag formulation, are important for a better prediction of helicopter cross-coupling behaviour. The delay causes, especially for pilot cyclic control inputs, an azimuthal shift in the effect of the aerodynamic coefficients. The control input becomes also slightly effective in the coupling axis and thus causing the coupling in helicopter response.

In order to capture the unsteady aerodynamic effects, approaches have been made that describe the aerodynamic phase lag as a pure low pass filter []. Although good improvements in helicopter cross coupling response could be achieved this approach can easily over-predict the effect since the achieved phase delay is not limited when increasing the low pass filter gain.

Therefore an additional physical based approach basing on Wagner's lift deficiency function is introduced to the finite unsteady state model. A similar formulation was used before in combination with the Pitt&Peters model [2] where satisfying improvements in helicopter cross-coupling response could be achieved.

### Finite State Unsteady Wake Model

In the finite state unsteady wake formulation presented by He and Peters, the inflow is expanded in terms of higher harmonic functions for azimuthal distribution and radial shape functions using Legendre polynomial functions. The resulting set of equations governing the dynamic inflow states are driven by the present (arbitrary) blade lift

distribution. A major advantage is that the number of harmonic and shape functions and thus the number of coefficients can be defined by the user in dependence of the particular application which makes the model well suited for a wide range of different investigations.

The Finite State Unsteady Wake Model bases on a pressure perturbation function  $\Phi$ , describing an acceleration potential in an incompressible potential flow field. The pressure function can be splitted into a convection part  $\Phi^V$  and an acceleration part  $\Phi^A$ :

$$\Phi = \Phi^V + \Phi^A \quad (1)$$

The convection part describes the pressure variation along the flow line, whereas the acceleration or unsteady part counts for the variation with time. Both pressure function parts satisfy the Laplace's equations.

When expressing the Laplace equations in ellipsoidal coordinates and expanding them with Legendre polynomial functions an analytical solution for the pressure function can be found:

$$\Phi = -\frac{1}{2} \sum_{m=0}^{\infty} \sum_{\substack{n=m+1, \\ m+3, \dots}}^{\infty} \bar{P}_n^m(\nu) \cdot \bar{Q}_n^m(i\eta) \cdot \left( \tau_n^{mc}(\bar{t}) \cos r\psi + \tau_n^{ms}(\bar{t}) \sin r\psi \right) \quad (2)$$

where  $\bar{P}_n^m$  and  $\bar{Q}_n^m$  denote the normalized associated Legendre functions of the first and second kind. The arbitrary cosine and sine coefficients  $\tau_n^{mc}$  and  $\tau_n^{ms}$  are functions of the present disk loads and thus vary with time. The index  $m$  denotes the respective harmonic number and  $n$  the mode shape related to harmonic  $m$ . The Legendre functions are defined only for  $n \geq m$ .

The normal component of the induced velocity  $w$  at the rotor disk can be expressed in a similar way as the pressure function using Fourier and Legendre functions:

$$w = \sum_{r=0}^{\infty} \sum_{\substack{j=r+1, \\ r+3, \dots}}^{\infty} \Psi_j^r(\nu) \cdot \left( \alpha_j^r(t) \cos r\psi + \beta_j^r(t) \sin r\psi \right) \quad (3)$$

where  $\alpha_j^r$  and  $\beta_j^r$  are the inflow states with respect to shape function  $\Psi_j^r$ .

Combining equations (1), (2) and (3) leads to an equation system for the inflow coefficients:

$$M \cdot \alpha_j^r + \left( \hat{L}_{jn}^{r,ms} \right)^{-1} \cdot V \cdot \hat{\alpha}_j^r = \frac{1}{2} \tau_n^{mc} \quad (4)$$

$$M \cdot \beta_j^r + \left( \hat{L}_{jn}^{r,cs} \right)^{-1} \cdot V \cdot \hat{\beta}_j^r = \frac{1}{2} \tau_n^{ms} \quad (5)$$

with a mass matrix:

$$M = \frac{2H_n^m}{\pi}, \quad H_n^m = \frac{(n+m-1)!(n-m-1)!!}{(n+m)!!(n-m)!!} \quad (6)$$

and a diagonal matrix  $V$  describing the free stream velocity  $V_\infty$  in the main diagonal.

Further  $\hat{L}_{jn}^{r,ms}$  and  $\hat{L}_{jn}^{r,cs}$  are the gain matrices having elements which are integral functions of the form:

$$\hat{L}_{jn}^{r,mc} = \frac{1}{\delta\pi} \int_0^{2\pi} \int_0^1 \bar{P}_j^r(\nu_0) \cos r\psi \cdot \int_0^\infty \frac{\partial}{\partial z} \left( \bar{P}_n^m(\nu) \bar{Q}_n^m(i\eta) \right) \cos m\psi \, d\xi d\nu d\psi \quad (7)$$

$$\hat{L}_{jn}^{r,ms} = \frac{1}{\pi} \int_0^{2\pi} \int_0^1 \bar{P}_j^r(\nu_0) \sin r\psi \cdot \int_0^\infty \frac{\partial}{\partial z} \left( \bar{P}_n^m(\nu) \bar{Q}_n^m(i\eta) \right) \sin m\psi \, d\xi d\nu d\psi \quad (8)$$

with  $\delta = 2$  for  $r = 0$  and  $\delta = 1$  for  $r \neq 0$ .

The theory can be refined by using a diagonal mass flow matrix  $V_n^m$  instead of  $V$  in equation (4) and (5), consisting of the equivalent velocity:  $V_1^0 = V_M$  and the steady state velocity:  $V_n^m = V_T$ , ( $m \neq 0, n \neq 1$ ) elements on its main diagonal. The velocity functions are derived as:

$$V_T = \sqrt{\mu^2 + \lambda^2} \quad \text{and} \quad V_M = V_T + \frac{\lambda\lambda_m}{V_T} \quad (9)$$

with:

$$\lambda_m = \frac{\sqrt{3\pi}}{2} \bar{\alpha}_1^0 \quad (10)$$

In addition, the obtained  $L$  matrix, the flow states and pressure coefficients are normalized with the factor  $2\sqrt{H_n^m}/\pi$  which then finally leads to:

$$\left( \bar{L}_{jn}^{r,mc} \right) \cdot \bar{\alpha}_j^r = -V_n^m \cdot \bar{\alpha}_j^r + \left( \bar{L}_{jn}^{r,mc} \right) \cdot \bar{\tau}_n^{mc} \quad (11)$$

$$\left( \bar{L}_{jn}^{r,ms} \right) \cdot \bar{\beta}_j^r = -V_n^m \cdot \bar{\beta}_j^r + \left( \bar{L}_{jn}^{r,ms} \right) \cdot \bar{\tau}_n^{ms} \quad (12)$$

The matrices  $\bar{L}$  consist of a time independent part (which can be calculated in advance) and a time varying part depending on the present wake skew angle. In hover and axial flight the  $\bar{L}$  are pure diagonal matrices, whereas in forward flight,

numerous elements are non zero and thus provide an "interstate" coupling between the individual inflow states.

### Generalized forces

Equations (11) and (12) are governed by the generalized forces, represented by the pressure coefficients  $\tau_n^m$ . For a lifting line or blade element theory they can be calculated as:

$$\bar{\tau}_n^{m c} = \frac{1}{\delta\pi} \sum_1^{N_b} \sum_1^{N_e} \frac{F_{b,e}}{\rho\Omega^2 R^4} \cdot \frac{\bar{P}_n^m(\nu)}{\nu} \cdot \sqrt{\frac{\pi}{4H_n^m}} \cdot \cos m\psi_b \quad (13)$$

$$\bar{\tau}_n^{m s} = \frac{1}{\pi} \sum_1^{N_b} \sum_1^{N_e} \frac{F_{b,e}}{\rho\Omega^2 R^4} \cdot \frac{\bar{P}_n^m(\nu)}{\nu} \cdot \sqrt{\frac{\pi}{4H_n^m}} \cdot \sin m\psi_b \quad (14)$$

where  $F_{b,e}$  is the lift of the particular blade element.

### Unsteady Aerodynamics

Theodorsen has formulated a theory which takes into account the unsteady aerodynamic effects experienced by an oscillating thin airfoil. Shed vortices in the near wake generated as an effect of the airfoil circulation time derivative cause the aerodynamic states (at the airfoil) to be delayed as a function of the oscillatory frequency. However, for practical use in helicopter rotor dynamics, the Theodorsen's theory is less applicable since it is formulated in the frequency domain and for a quasi steady free stream flow velocity.

Therefore in the present case the implementation of the more general formulations of Küssner and Wagner for sharp edge gusts and oscillating airfoils, respectively, is found to be more convenient. Especially Wagner's theory is of interest in order to describe the unsteady rotor blade aerodynamic effects due to shed vortices in the near wake as a result of circulation variations with time.

Wagner's function  $\phi_{step}(t^*)$  describes the aerodynamic circulatory airfoil lift response to a step change in the distribution of the velocity normal to the airfoil in an incompressible and inviscid flow environment.

**Figure 5** shows the Wagner function in dependence of the reduced time:

$$t^* = \frac{2}{c} \int_0^t U_\infty(\tau) d\tau \quad (15)$$

in terms of half chords travelled through the surrounding air (which is in general a time dependant function). And  $U_\infty$  containing all effects which contribute to the local airfoil section free stream velocity components (i.e. global free velocity and total blade motion).

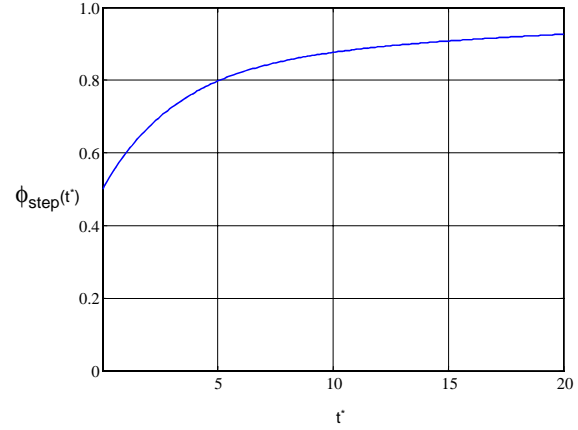


**Figure 5:** Wagner's function

An approximation to Wagner's function is given by R.T. Jones and can be written in terms of an exponential series with 4 parameters:

$$\phi_{step}(t^*) \approx 1 - a_1 \cdot e^{-b_1 t^*} - a_2 \cdot e^{-b_2 t^*} \quad (16)$$

with the standard values of  $a_1 = 0.165$ ,  $a_2 = 0.335$ ,  $b_1 = 0.041$  and  $b_2 = 0.320$  (see [8]). Note that  $a_1 + a_2 = 0.5$  which corresponds to the exact Wagner result for  $t^* = 0$ . The coefficients  $a$  and  $b$  can be adapted to the actual airfoil as shown in [9] for the BO105 NACA 23012 airfoil. In this work the coefficients are optimised for the particular airfoil using parameter identification tools. However, for a more general application, e.g. other airfoils on other helicopter types, the standard parameter set as mentioned above is used.

For practical use the Wagner step response has to be expressed in a more general manner as a differential equation which can be driven by arbitrary changes in angle of attack and free stream velocity. For this, equation (16) is transformed from the reduced time domain into the frequency domain using Laplace's transformation. Here, the step input can be eliminated from the obtained transfer function by multiplication with  $s$  which results in:

$$\phi(s) = \phi_{step}(s) \cdot s = \frac{1 + D_1 \cdot s + W_1 \cdot s^2}{1 + D_2 \cdot s + W_2 \cdot s^2} \quad (17)$$

The coefficients  $D$  and  $W$  directly depend on the  $a$  and  $b$  coefficients in (16). From (17) a differential equation in the reduced time domain can be derived:

$$W_2 y'' + D_2 y' + y = W_1 x'' + D_1 x' + x \quad (18)$$

where  $x$  denotes the input and  $y$  the output signal. After short reformulation and substitution of the  $a$  and  $b$  coefficients a first order ODE system in the reduced time domain is obtained:

$$\begin{aligned} x_1' &= -x_2 + (a_1 b_1 + a_2 b_2) \cdot x \\ x_2' &= b_1 b_2 \cdot x_1 - (b_1 + b_2) \cdot x_2 + (a_1 b_1^2 + a_2 b_2^2) \cdot x \\ y &= x_1 + (1 - a_1 - a_2) \cdot x \end{aligned} \quad (19)$$

To transform this system into a state space form described in the 'normal' time domain the derivative of equation (15) is used:

$$t^* = \frac{2}{c} \int_0^t U_\infty(\tau) d\tau \Rightarrow dt^* = \frac{2U_\infty(t)}{c} dt \quad (20)$$

and thus:

$$\left( \cdot \right)' = \frac{d(\cdot)}{dt^*} = \frac{d(\cdot)}{dt} \cdot \frac{c}{2U_\infty} = \left( \dot{\cdot} \right) \cdot \frac{c}{2U_\infty} \quad (21)$$

which applied to (19) gives:

$$\begin{aligned} \begin{pmatrix} \dot{x}_1 \\ \dot{x}_2 \end{pmatrix} &= \frac{2U_\infty}{c} \cdot \begin{bmatrix} 0 & -1 \\ b_1 b_2 & -b_1 - b_2 \end{bmatrix} \cdot \begin{pmatrix} x_1 \\ x_2 \end{pmatrix} + \\ &+ \frac{2U_\infty}{c} \cdot [a_1 b_1 + a_2 b_2 \quad a_1 b_1^2 + a_2 b_2^2] \cdot x \\ y &= [1 \quad 0] \cdot \begin{pmatrix} x_1 \\ x_2 \end{pmatrix} + [1 - a_1 - a_2] \cdot x \end{aligned} \quad (22)$$

For use in the calculation of unsteady aerodynamic blade loads equation (22) is driven by the instantaneous angle of attack at  $\frac{3}{4}$  chord as well as the local instantaneous free stream velocity. Both quantities can be combined elegantly in the velocity normal to the airfoil chord, i.e.  $V_z$ :

$$V_z = U_\infty \cdot \sin \alpha \quad (23)$$

which results in an effective normal velocity  $V_{z,e}$ .

The formulation of (22) is able to represent the effects on the circulatory lift coefficient of an airfoil in an oscillating free stream velocity as described by Leishman and van der Wall in [8] using a recursive approach.

It has to be mentioned that the non-circulatory parts of the lift function are not taken into account in the present formulation. Their contribution is of one order less than the circulatory effects for the essential frequencies incorporated in helicopter flight dynamic applications.

## Compressibility

To take account for compressibility effects a relatively simple but accurate approach can be used which makes use of a factor depending on the local free stream Mach number:

$$\beta = \sqrt{1 - \frac{U_\infty^2}{a_s^2}} \quad (24)$$

The square of this factor is multiplied to the  $b$ -coefficients in the expression given in (16). For use in rotor aerodynamics the parallel and perpendicular flow Mach numbers are taken:

$$M_x = \frac{U_\infty}{a_s} \cdot \cos \alpha \quad \text{and} \quad M_z = \frac{U_\infty}{a_s} \cdot \sin \alpha \quad (25)$$

where  $a_s$  denotes the speed of sound. The equation system of (22) is then 2 times evaluated (for  $M_x$  and  $M_z$  resp.) using the compressibility factor:

$$\begin{aligned} \begin{pmatrix} \dot{x}_1 \\ \dot{x}_2 \end{pmatrix} &= \frac{2U_\infty}{c} \cdot \begin{bmatrix} 0 & -1 \\ \beta^4 (b_1 b_2) & \beta^2 (-b_1 - b_2) \end{bmatrix} \cdot \begin{pmatrix} x_1 \\ x_2 \end{pmatrix} \\ &+ \frac{2U_\infty \beta^2}{c} \cdot [a_1 b_1 + a_2 b_2 \quad \beta^2 (a_1 b_1^2 + a_2 b_2^2)] \cdot M_{x,z} \end{aligned} \quad (26)$$

$$M_{ex,z} = [1 \quad 0] \cdot \begin{pmatrix} x_1 \\ x_2 \end{pmatrix} + [1 - a_1 - a_2] \cdot M_{x,z}$$

Finally, the effective angle of attack (due to circulatory effects) and the effective Mach number (e.g. for use in a table look up scheme) can be expressed as:

$$\alpha_e = \tan^{-1} \left( \frac{M_{z,e}}{M_x} \right) \quad \text{and} \quad M_e = \sqrt{M_{x,e}^2 + M_{z,e}^2} \quad (27)$$

It is important to use  $M_x$  and not  $M_{x,e}$  in the calculation of the effective angle of attack!

The phase delay of the effective angle of attack  $\alpha_e$  with respect to the quasi steady angle  $\alpha$  is particularly dependant on the phase between free stream velocity oscillation  $U_\infty(t)$  and the  $\alpha$  oscillation itself. It was found that for a 180° shift between both oscillations (what is more or less the case for a helicopter in forward flight) the  $\alpha_e$  phase delay is minimal.

**Figure 6** shows this effect for an airfoil section of the EC135 helicopter in a 30 kts level flight. The solid line denotes the quasi-steady angle of attack and the dotted line the resulting effective angle as a function of the rotor azimuth  $\psi_b$  starting from the rear blade position. The phase shift due to unsteady aerodynamics was estimated with 1.5°, whereas the

hover case which is shown in **figure 7** shows a phase shift of about  $7^\circ$ . However, amplitudes are very small here.

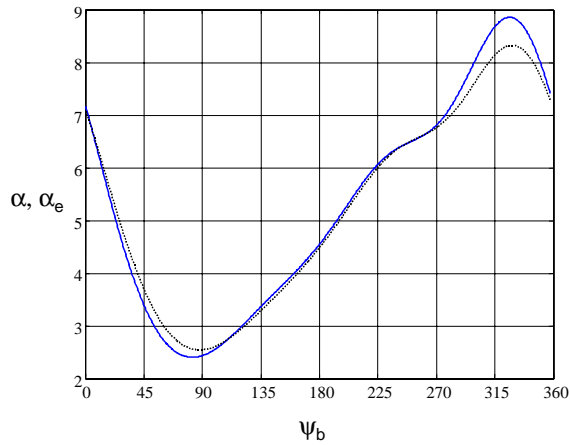


**Figure 6:** effective angle of attack for EC135 airfoil section at 30 kts level flight

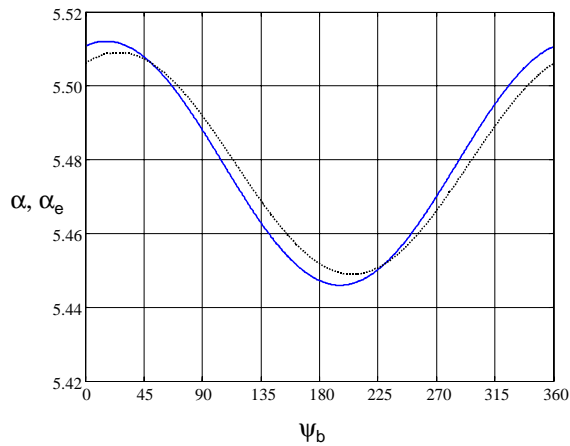


**Figure 7:** effective angle of attack for EC135 airfoil section in hover

For both figures the induced down wash is calculated using the finite state unsteady wake formulation with 4 harmonics. In **figure 6** the dent in the angle of attack at about  $240^\circ$  of azimuth, caused by the 2<sup>nd</sup> harmonic distribution of the finite state unsteady wake formulation. This effect could not be observed when using the first harmonic Pitt&Peters model

## System Identification

The estimation of a reliable rotorcraft derivative model from flight data is hindered mainly by the deteriorated signals from high vibrations, helicopter instabilities and modeling complexities of rotor/fuselage system. Additionally, rotorcraft dynamics generally exhibit high degree of inter-axis coupling. A 6 DOF rigid body model is the minimum required to adequately predict the helicopter dynamics in low and mid frequency

range, e.g., for applications with a limited bandwidth such as flying qualities evaluation and pure stabilization purposes. For a more reliable representation of higher frequency dynamics, e.g., the design of a model-following control system for in-flight simulation purposes, a higher order model formulation which covers higher bandwidth is necessary.

In order to establish the tools and to gain experience necessary for identifying this kind of models for the EC135 helicopter as soon as appropriate FHS flight test data will be available, the system identification procedure is applied using EC135 off-line simulation data [10].

## Model structure

One approach to improve the prediction capabilities of 6 DOF models at higher frequencies is to formulate extended models which include the rotor degrees of freedom, either in an explicit second order form or in a first order approximation. The latter approach has shown to be sufficient accurate for catching the effects of rotor degrees of freedom [11].

Selection of an appropriate mathematical model structure (i.e. incorporated states) is a crucial step in system identification which affects both the complexity and the utility of the identified model. Besides, models with linear aerodynamics and 6 DOF nonlinear rigid body kinematics and gravity terms, 8 DOF models are derived by extending them with additional two states representing the longitudinal and lateral rotor flapping.

During the model identification process, a decision on the selection of parameters for entry into the estimation model is required, since not all derivatives have an equal impact on the fidelity of rotorcraft response. One approach to recognize and retain only significant parameters in the estimation model is based on the Cramer Rao Bounds (CRB) of the derivatives. The CRB of the identified parameters are obtained from the information matrix which is anyway computed by the output error algorithm during the estimation process. Derivatives which are secondary in nature and show exceptionally high standard deviations are dropped (fixed to zero) from estimation at each model iteration step.

## Data generation

Due to the fact that real flight test data of EC135 helicopter are not available yet, the data to be analyzed are generated from the DLR's nonlinear helicopter simulation environment SIMH. For this investigations the fully non-linear simulation model

described before, configured for a EC135, is used. Configuration data and especially the aerodynamic models were provided by the manufacturer ECD and a cross-check with their simulation environment has been performed. Up to now this incorporates, however, the basic and thus simplified engine and fenestron dynamic description. As soon as appropriate FHS flight test data will be available the identification task will be efficiently accomplished again, using the experience gained in this investigations.

Data are generated for hover and at 30 m/s and 45 m/s level flight at a pressure altitude of 2250 m. After establishing trim at each of the defined flight conditions, a multistep modified 3-2-1-1 input with a total time length of 7 seconds is applied to generate the helicopter dynamic responses which is shown in **figure 8** for the 30 m/s case. Within one maneuver, only one control input is used to excite the on-axis response. At the end of the input, the controls are held constant for some time to permit the natural response of the rotorcraft to be recorded. The model is then retrimmed to the initial condition and a repeat maneuver is performed with the same control now applied in the opposite direction, in order to increase the data information content.

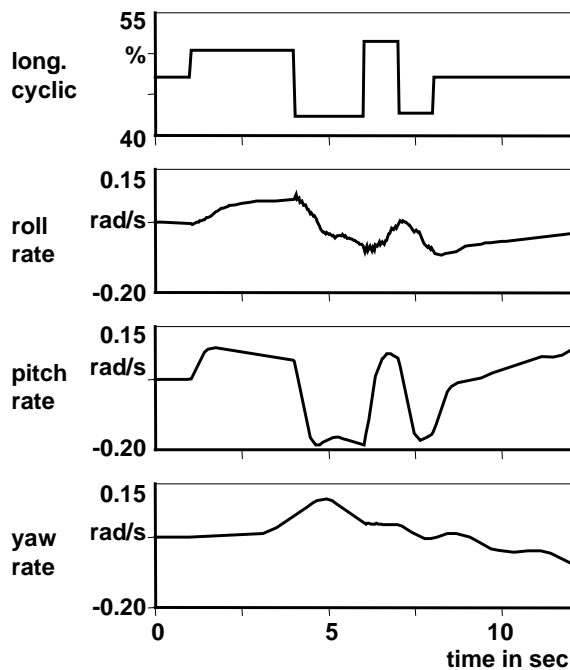


**Figure 8:** longitudinal 3-2-1-1 EC135 at 30 m/s

### Identification method

In the present work the parameter estimation software tool ESTIMA, a development of DLR's institute of Flight Research, is used [12]. The software incorporates various advanced parameter estimation techniques like filter error method and extended Kalman filter besides the classical output

error and least square methods. It can be applied to both linear and nonlinear systems and can handle large amount of data and allows for the analysis of multiple concatenated runs. Here, an output error method in time-domain is used which also happens to be the default option of optimization method in ESTIMA. The output error approach is based on maximum likelihood technique that accounts for measurement noise, but neglects process noise.

### Identification results

A comparison of the identified derivative values of the 6 DOF and 8 DOF models shows that due to the presence of flapping states in the estimation model, the dynamic behaviour described by the primary rigid body derivatives is now produced by the rotor flapping derivatives. This is logical since the pilot controls are acting on the rotor and the rotor response then excites the rigid body motion.

In principle, the extended model is generally not expected to produce a higher accuracy in low frequency range than that of the 6 DOF model. But it is definitely expected to provide a better fit in response at higher frequencies, e.g. for the short term response of pitch and roll accelerations, particularly where the step changes in the control input are applied.

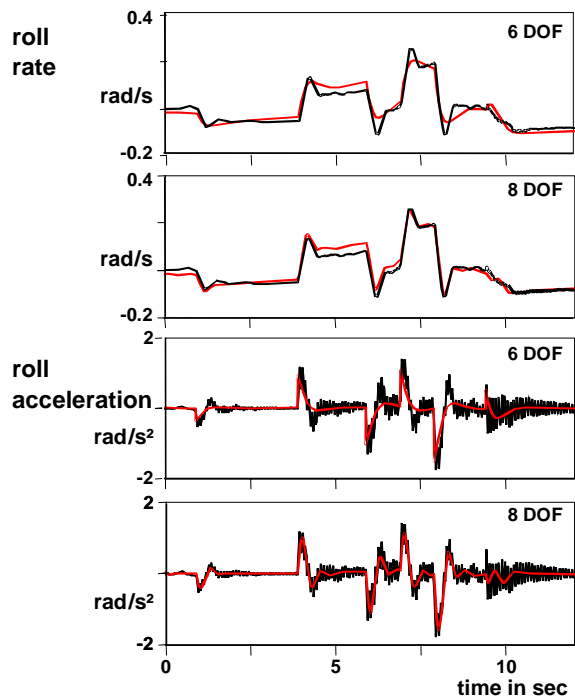


**Figure 9:** on-axis roll response in hover

As an example of the fidelity of the estimated system, comparisons between the on-axis hover roll (depicted by the black solid line) and the 6 DOF and 8 DOF identified models (light red line) are shown in **figure 9**. As can be seen from the acceleration as

well as in the rate plots, both 6 DOF and 8 DOF models match quite well the low frequency over all response. However, the 8 DOF description is also capable of predicting the high frequencies and transients which are particularly important in the high bandwidth control system design.

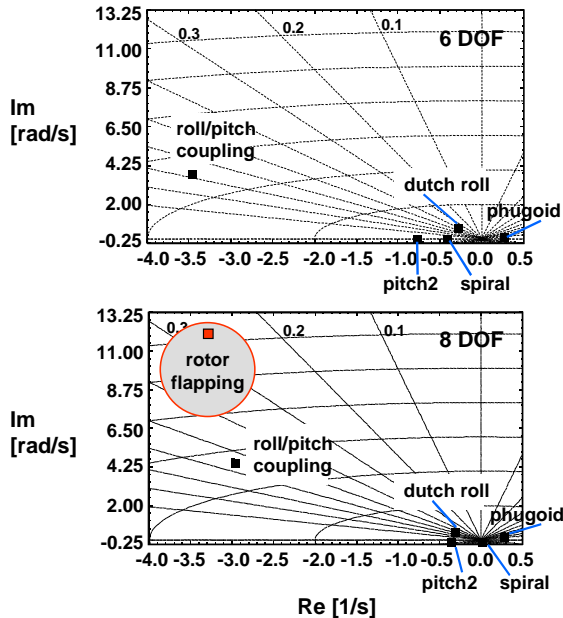


**Figure 10:** stability plots for EC135 in hover

In addition, since the data set was destined for control system boundary tests, simulation was performed using an extreme aft cg configuration.

The stability plots for the identified EC135 models are shown in **figure 10**. Instead of a classic roll and pitch damping mode the simulated EC135 exhibits a roll/pitch coupling in both 6 DOF and 8 DOF models. The phugoid mode is unstable and the spiral mode shows increased divergence at higher speeds. The additional high frequency complex pole from the identified 8 DOF model represents the flapping mode. This mode allows the high frequency transient responses as shown in **figure 9**.

### Control System Design

The current FHS control system design and development is committed to the FHS final certification tests. In this context the first control system application consists of a direct 1:1 feed through of the pilot controls, with in addition the option of generating different additional erroneous control inputs, e.g. spikes, runaways, delays, etc. The parameters and particular options can be selected and adjusted by the pilot or flight test engineer on their control and display unit (CDU) fitting to the particular tests to be performed.

This application was used in preliminary system tests on ground in fall 2000 at DLR aimed to get a detailed insight into the complex interaction of the core and experimental system, especially from an operational or safety point of view. In the current ongoing final certification phase these implemented tools are again applied in ground as well as flight tests.

For the implementation of this application the software structure and hard/software interfaces between the control system implemented on the experimental computer and its outside world (e.g. core system interface computer, data management computer, sensors) have been defined and established. These structures and interfaces form the basis of all future control system software developments such as the MFCS.

One of the test items during the certification phase is to check the safety procedure of taking over by the safety pilot the helicopter command either by control force override or switch activation. For the realisation of these tests it is specified that the evaluation pilot is provided with control system characteristics that differ noticeably from the basic control dynamics. This allows to check the correct synchronisation, mode switching and transient behaviour when changing the command from one pilot to the other.

To realise the demands for changing the control characteristics as described above, a pure feed-forward control system, as shown (for the roll and pitch axes only) in **figure 11**, is implemented. The control system in this configuration consists of 3 separated blocks in the feed-forward branch for each control axis.

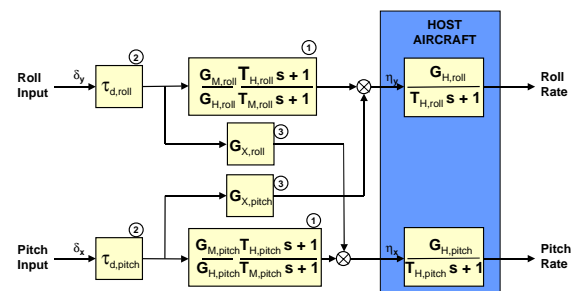


**Figure 11:** feed-forward control system

The parameters to describe the equivalent 1<sup>st</sup> order system dynamics of the host aircraft block at the right hand side are evaluated from the identified 8 DOF EC135 models, presented in the previous paragraph. Table 1 shows the damping and control parameters for hover, 30 m/s forward flight and 45 m/s forward flight.

The first control system block consists of a classic lead/lag filter description. The numerator is to cancel the equivalent 1<sup>st</sup> order system dynamics of the host helicopter in the right hand side block. The denominator then defines the desired 1<sup>st</sup> order dynamics, in terms of damping and controllability.

	0 m/s	30 m/s	45 m/s
$L_p$	12.3	8.4	7.5
$L_{\delta_y}$	0.22	0.19	0.19
$M_q$	4.1	3.7	3.7
$M_{\delta_x}$	0.11	0.11	0.10

**Table 1:** damping and control derivatives

The second block introduces a pure transport delay to the pilot commands. Finally the third block consists of a static cross-feed gain with respect to the other control axis. The representation of the 1<sup>st</sup> order system dynamics as shown in **figure 11**, using gain and time constant parameters can easily be related to the flight mechanic description which makes use of damping and control derivatives by using equation (28):

$$\frac{p}{\delta_y} = \frac{L_{\delta_y}}{L_p + s} = \frac{G_{H,roll}}{T_{H,roll} \cdot s + 1}, \quad (28)$$

here shown for the roll axis only.

In order to show the effect of the damping and time delay adjustment the bandwidth criterion as specified in the Aeronautical Design Standard 33 (ADS-33E [13]) is used. The ADS-33E specification contains requirements for evaluating helicopter handling qualities. The bandwidth criterion allows to quantify the helicopter short term response to control inputs (e.g. [14]).

In **figure 12** the roll bandwidth  $\omega_{bw}$  and equivalent time delays  $\tau_p$  for the FHS helicopter for 3 different forward speeds are shown. To the system inherent delays of the basic EC135 a control system delay  $\tau_c$  of 40 ms is already added. The 40 ms are the maximum delay between pilot control inputs and actuator position as defined in the FHS specifications.

As can be seen for all velocities the EC135 roll bandwidth handling qualities lie well within the level 1 boundaries. Here the boundaries for a target acquisition and tracking task are displayed which are generally tighter than the regular bounds.

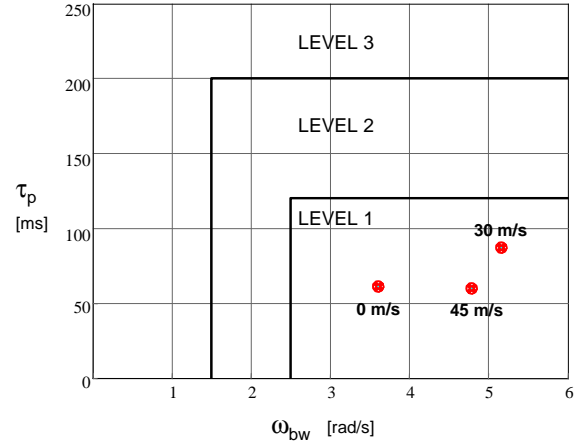


**Figure 12:** roll bandwidth and equivalent time delay

The pitch bandwidth and time delays are presented in **figure 13**. Here also an additional control system delay of 40 ms is used. Again, for all 3 investigated velocity cases level 1 handling qualities can be reached with respect to the target acquisition and tracking boundaries.

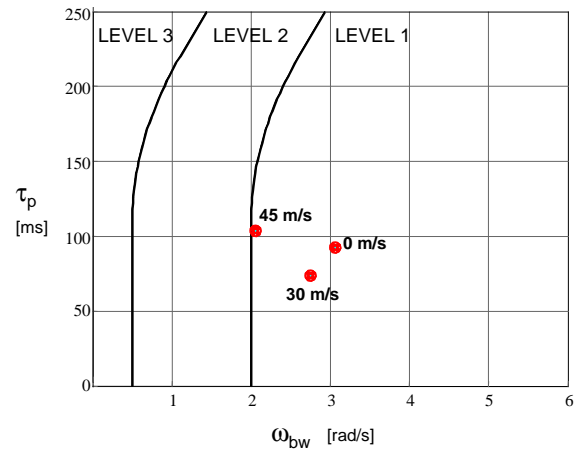


**Figure 13:** pitch bandwidth and equivalent time delay

By adjusting the desired system damping in terms of changing time constant  $T_M$  and introducing an additional transport delay  $\tau_d$  the bandwidth and equivalent time delay can be influenced as depicted in **figure 14**. By decreasing the damping coefficient and thus making the system less agile, handling qualities can be easily shifted to level 2 or even level 3. The same effects occur when the additional transport delay is increased. For high  $\tau_d$  ( $> 150$  ms) the system is degraded to level 3 and the pilot will easily experience PIO tendencies. In contrast, an increase of the damping coefficient leads in this open loop structure to a system which is faster than the basic system. However, due to the higher necessary control activity the system suffers more likely from actuator rate saturation. In the present investigations an estimation of the actuator rate

saturation was performed, represented by the open circles in case of occurrence.

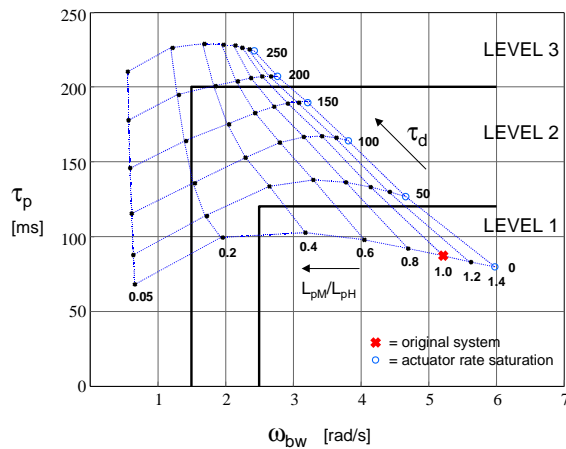


**Figure 14:** roll damping and transport delay variation

The pitch bandwidth and equivalent time delay diagram is shown in **figure 15**. Again the damping and transport delay are varied changing the basic system characteristics. Also in the pitch axis the system can be degraded to level 2 or even level 3 when using low damping coefficients and high transport delays.

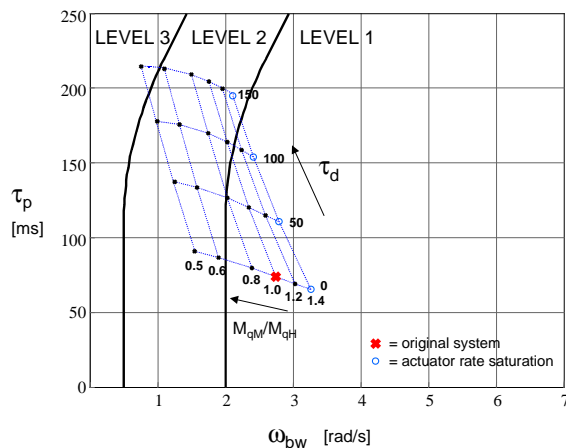


**Figure 15:** pitch damping and transport delay variation

The cross-feed gains from **figure 11** are evaluated and optimised using the coupling criterion, specified in the ADS-33E. This criterion predicts the handling qualities for high frequency tasks such as the slalom tracking task [15]. From **figure 16** it can be seen that the basic helicopter with zero cross-feed gains has level 2 handling qualities with respect to pitch-roll and roll-pitch coupling behaviour. Especially the roll-due-to-pitch coupling is very distinctive, due to the low roll inertia moment and strong coupling

dynamics incorporated in the bearingless main rotor design of the EC135.

When optimising the static cross-feed gains the coupling handling qualities level can be reduced close to the level 1 boundary. Actually, a constant gain can only be optimal for one frequency. The coupling criterion, however, rates an average coupling level. Therefore, static cross-feed gains are not the appropriate measure to improve coupling handling qualities for strongly coupled helicopters.

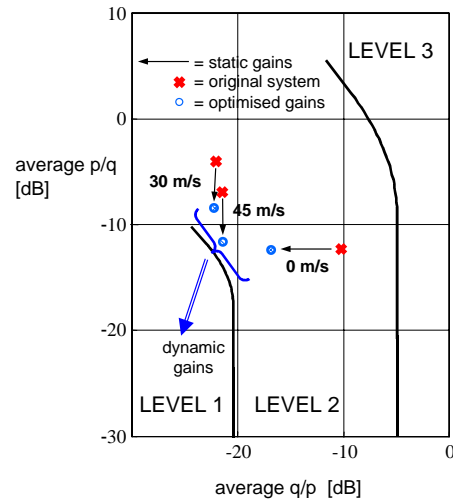


**Figure 16:** representation of the coupling criterion

In ongoing and future investigations the dynamic cross-feed provided by the MFCS will be used. The MFCS is capable of cancelling out nearly all cross-coupling dynamics as has been shown previously for the ATTHes inflight simulator.

Although the first control system applications presented here remain 'simple' in structure they are very helpful and effectively useable in the FHS certification test phase. Moreover, the feed-forward implementation as shown in **figure 11** can also be used in first handling qualities open loop investigations as soon as the FHS comes into operation.

Finally, the control system structure and interfaces established in this first applications and the experience gained working with a complex system such as the FHS, will definitely contribute to the ongoing MFCS development and investigations.

## Conclusions

An overview of the chain of tools and disciplines necessary for the experimental control system design process is presented. An accurate non-linear, generic simulation model is found to play an important role this process. In order to improve the simulation

fidelity, especially for high bandwidth applications, additional model extensions, representing the local unsteady aerodynamic effects, are implemented and tested.

The off-line simulation environment is used to generate data suitable for system identification purposes. From this data 6 DOF and extended 8 DOF models incorporating rotor flapping degrees of freedom are identified. It is shown that especially the 8 DOF models are able to predict the typical helicopter response behaviour including the high frequency transient responses for sharp edged control inputs.

Finally, the first experimental control system applications are presented. They consist of a lead-lag filter as a pure feed-forward in the pilot control branch. Their applicability is shown by means of handling qualities criteria specified in the ADS-33E.

The experience gained with the complex interaction of the experimental and overall system will definitely help in the development of the MFCS.

## References

- [1] H.J. Pausder, U. Butter, F. Steinmaier, "ACT/FHS for the Next Generation Technologies Evaluation and Demonstration", 25<sup>th</sup> European Rotorcraft Forum, Rome, Italy, September 14-16, 1999
- [2] M. Hamers, W. von Grünhagen, "Nonlinear Helicopter Model Validation Applied to Realtime Simulations", American Helicopter Society 53<sup>rd</sup> Annual Forum, Virginia Beach, Virginia, April 29 - May 1, 1997
- [3] Ph. Krämer and B. Gimonet, "Improvement of Nonlinear Simulation Using Parameter Estimation Techniques", 26<sup>th</sup> European Rotorcraft Forum, The Hague, The Netherlands, September 26-29, 2000
- [4] M. Hamers and P.M. Basset, "Application of the Finite State Unsteady Wake Model in Helicopter Flight Dynamic Simulation", 26<sup>th</sup> European Rotorcraft Forum, The Hague, The Netherlands, September 26-29, 2000
- [5] P.M. Basset, O. Heuze, J.V.R. Prasad and M. Hamers, "Finite State Rotor Induced Flow Model for Interferences and Ground Effect", American Helicopter Society 57<sup>th</sup> Annual Forum, Washington, DC, May 9-11, 2001
- [6] D.A. Peters, D.D. Boyd and C.J. He, "Finite-State Induced-Flow Model for Rotors in Hover and Forward Flight", American Helicopter Society 43<sup>rd</sup> Annual Forum, St. Louis, Mo., April 18-20, 1987
- [7] H. Mansur and M.B. Tischler, "An Empirical Correction Method for Improving Off-Axis Response Prediction in Component Type Flight Mechanics Helicopter Models", AGARD Flight Vehicle Integration Panel Symposium on "Advances in Rotorcraft Technology", Ottawa, Canada, May 27-30, 1996
- [8] J.G. Leishman, "Principles of Helicopter Aerodynamics", Cambridge Aerospace Series, Cambridge University Press, UK, 2000
- [9] B.G. van der Wall, "Analytische Formulierung der Instationären Profilbeiwerte und deren Anwendung in der Rotorsimulation", Research Report, FB 90-28, DLR Braunschweig, 1990
- [10] J. Singh, R.V. Jategaonkar and M. Hamers, "EC135 Rotorcraft System Identification: Estimation of Rigid Body and Extended Models from Simulated Data", DLR Internal Report, IB 2000-31, DLR Braunschweig, 2000
- [11] J. Kaletka and W. von Grünhagen, "Identification of Mathematical Models for the Design of a Model Following Control System", Vertica, Vol. 13, No. 3, 1989, pp.213-228.
- [12] R.V. Jategaonkar, "ESTIMA : A Modular and Integrated Software Tool for Parameter Estimation and Simulation of Dynamic Systems – User's Manual, Version 1.0", DLR Internal Report, IB 2001-29, DLR Braunschweig, 2001
- [13] "Handling Qualities Requirements for Military Rotorcraft", Aeronautical Design Standard Performance Specification, ADS-33E-PRF, March 21, 2000
- [14] H.J. Pausder and C.L. Blanken, "Investigations of the Effects of Bandwidth and Time Delay on Helicopter Roll-Axis-Handling Qualities", Piloted Vertical Flight Aircraft. A Conference on Flying Qualities and Human Factors, San Francisco, Ca, January 20-22, 1993
- [15] C.J. Ockier, H.J. Pausder and C.L. Blanken, "An Investigation of the Effects of Pitch-Roll (De)-Coupling on Helicopter Handling Qualities", Research Report, FB 95-08, DLR Braunschweig, 1995